Sea Effects on Grounding Systems An Analytical and Numerical Study

A.S. Bretas, *University of Florida, USA*, and R. Andolfato – D. Cuccarollo, *SINT Ingegneria, Italy*

***Abstract*-- The interest on grounding system analysis is related to the increasing demand on the safety of power systems. A well designed grounding system can ensure reliable operation of power systems and the safety of human beings in fault conditions. The relevance of the problem is increasing with increasing short circuit fault currents and also with the power systems expansion. Grounding systems close to the seacoast are very common in case of industrial or power plants. It is reasonable to suppose that the sea, with its large volume and its low resistivity, can affects the GPR "Ground Potential Rise" and the touch and step voltages distribution of a grounding system. However, it is not evident how and how much. It is easy to guess that the GPR tends to decrease due to the effect of the sea, but it is quite surprising to see that despite this, the touch and step voltages tend to increase and that close to the seacoast, an otherwise safe grounding system can be dangerous for people. On the opposite, sea effects seem not relevant on conditions of insulated pipelines protected with cathodic protection plants. This paper presents an analytical and numerical study of this important issues not yet adequately reported in literature.**

***Index Terms*-- Grounding Systems, Earthing Systems, Cathodic Protection, Multilayer Soil Models, Computer Modelling, PEEC.**

I. Introduction

Grounding systems can be calculated using one of the suitable electromagnetic analysis methods (see [10] for a complete review). This work relates with some modules implemented in the XGSLab™ simulation environment [14], [15]. XGSLab™ is based on the so-called PEEC "Partial Element Equivalent Circuit" method, a numerical method with an high computational efficiency. The PEEC method can readily incorporate electrical components based on a circuit theory, such as impedances, transmission lines, cables, transformers, switches, and so on [10].

The XGSLab™ simulation environment may be applied in many engineering applications, as for instance: grounding, cathodic protection, electromagnetic fields and interferences, fault currents distribution and lighting. The program can consider systems over or below the soil surface and can work both in frequency and time-domain in a wide frequency range and also in non-stationary conditions. This so large application range is due to the very general calculation model adopted (based on Maxwell equations, Green functions and Sommerfeld integrals), which introduces a limited number of approximations.

In the Table I are listed the main aspects considered by XGSLab™. More details about the used calculation model are given in literature ([1], [2], [3], [4], [5], [6]).

TABLE I
Aspects taken into account in the used program

Resistive Coupling	Yes
Capacitive Coupling	Yes
Self-Impedance	Yes
Inductive Coupling	Yes
Soil Parameters	ρ, $\varepsilon = f(\omega)$
Propagation Law	$e^{-\gamma r}/r$

The simulation of underground systems represents one of the most usual applications of XGSLab™. As known, in this field the soil modelling represents one of the most crucial aspects. There is much literature about the criteria to set an appropriate soil model which can be used to predict the performances of a grounding system [5].

XGSLab™ allows you to use uniform, multilayer and multizone soil models (with an arbitrary layers or zones number) and takes into account not only soil resistivity but also soil permittivity and frequency dependence of soil parameters according to the most diffused models [7], [8], [12].

A uniform soil model should be used only when there is a moderate variation in apparent measured resistivity but, for the majority of the soils, this assumption is not valid.

The soil structure and the soil resistivity in general change both in vertical and horizontal direction (see Fig. 1.1) and only a 3D map gives an accurate description of real life conditions. This aspect is more evident close to the seacoast, because the effects of the sea, a media characterized by a very low resistivity.

The vertical changings are usually predominant than horizontal ones, but to correctly model soil conditions, it is essential to consider grounding system size.

In case of small systems, as for instance grounding systems with a size up to a few hundred meters, soil model is not significantly affected by horizontal changings in soil resistivity and usually a multilayer soil model is the most appropriate model [13]. The layers number depends on the soil resistivity

This work was supported by SINT Ingegneria Srl which allowed the use of the software XGSLab™ and provided the financial support.

variations in vertical direction. Literature states that the double layer soil model is adequate in about the 20% of cases, while in the 80% of cases a model with three or more layers is required [13].

In case of systems of intermediate size, as for example grounding systems with a size up to a few kilometers, soil model is affected by both horizontal and vertical changings in soil resistivity and usually an equivalent double or triple layer soil model is appropriate [13].

The parameters of the multilayer soil model can be calculated based on soil resistivity measurements [11].

In case of larger systems, soil model is usually significantly affected by horizontal changings in soil resistivity and a multizone soil model which takes this aspect into account is more appropriate than a multilayer soil model [14].

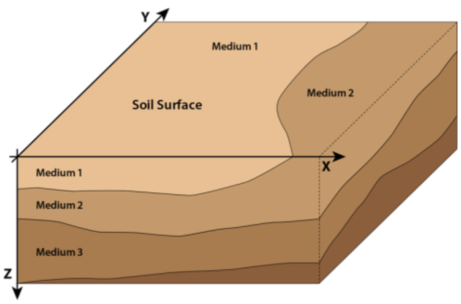

Fig. 1.1. A typical “real life” soil cross section

Close to the seacoast, soil have some unique characteristics. The sea resistivity is usually about 0.20 Ωm, thus much lower than the soil resistivity. The current spread to the earth by a grounding system close to the seacoast tends to flow towards the sea with relevant effects on GPR, earth surface potential and touch and step voltages distribution.

The sea can be represented as a large volume of low resistivity material at the potential of the remote earth, that is null. The sea effects can be simulated in a different way to the interfaces between layers. The sea effects can be represented with an upper surface corresponding to the interface air sea and a bottom surface corresponding to the seabed. The PEEC method using a suitable model, can simulate the sea effects in a very realistic way.

Multilayer soil model and seabed representation allow a very realistic simulation of grounding systems close to the seacoast. In particular, seabed and seacoast shapes can be chosen arbitrarily (see Fig. 1.2).

Still, multizone soil model allows a good simulation the seacoast suitable in case of very large systems. In this case, the seabed is assumed at an infinite depth (see Fig. 1.3).

The remainder of this paper is as follows. In the first theoretical part of the paper, a synthetic description of the implemented method is given together with its application limits and range. The second part is propaedeutic to the simulation of the sea and describes the simulation of an arbitrary low resistivity finite volume close to a grounding system. The differences of GPR, earth surface potential and touch and step voltages distribution without and with this volume (at floating or imposed to zero potential) are analyzed. The third part describes the simulation of the effects of the sea on a grounding system close to the seacoast. The soil is represented with a multilayer soil model and seabed is simulate in a realistic way. The differences of GPR, earth surface potential and touch and step voltages distribution without and with the presence of the sea are analyzed. The fourth part describes the simulation of the effects of the sea on a cathodic protection system with impressed current close to the seacoast. The soil and the sea are represented with a multizone soil model. The differences on protection conditions with and without the presence of the sea are analyzed.

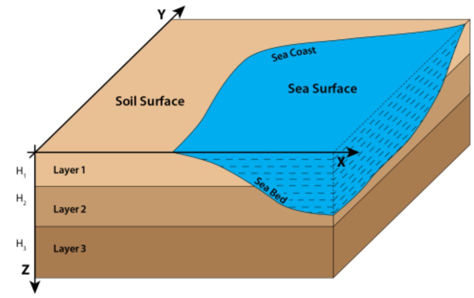

Fig. 1.2. Cross section of a multilayer soil model close to the seacoast

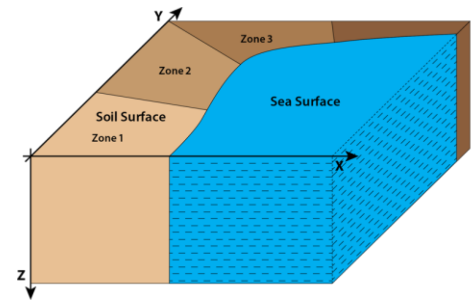

Fig. 1.3. Cross section of a multizone soil model close to the seacoast

II. THEORY

In the following, a short description of the model’s derivation and considered in this study are presented. The considered approach for this study is 3D space modelling. The conductor’s network is partitioned into small thin and straight elements (current and charge cells) [10].

Using the vector and scalar potentials, Maxwell equations can be written as in the following (Helmholtz equations):

$$\begin{cases} \Delta \mathbf{A} - \gamma^2 \mathbf{A} = -\mu \mathbf{J} \\ \Delta U - \gamma^2 U = -\dfrac{q}{\varepsilon} \end{cases} \tag{1}$$

where $\mathbf{A}$ (Vs/m) is the vector potential, U (V) is the scalar potential, $\gamma = \sqrt{j\omega\mu(\sigma + j\omega\varepsilon)}$ (1/m), σ (S/m) μ (H/m) and ε (F/m) are the propagation coefficient, conductivity, permeability and permittivity of the medium respectively, and q (C/m^3) and $\mathbf{J}$ (A/m^2) are charge and current density distribution on the sources respectively.

Solution of (1) for sources with linear current and charge density distribution are given by the following equations:

$$\begin{cases} A = \dfrac{\mu}{4\pi}\displaystyle\int_L I\,\dfrac{e^{-\gamma r}}{r}dl \\ U = \dfrac{1}{4\pi\varepsilon}\displaystyle\int_L q\,\dfrac{e^{-\gamma r}}{r}dl \end{cases} \tag{2}$$

where I (A) and q (C/m) are the current and charge density distribution respectively.

Maxwell equations give the following relation between electric field $\mathbf{E}$ (V/m) and scalar and vector potentials:

$$\mathbf{E} = -gradU - j\omega\mathbf{A} \tag{3}$$

where ω (rad/s) is the angular frequency.

Considering that the electric field and vector potential on the surface of a conductor are parallel to the conductor axis, (3) can be rewritten along the conductor axis as follows:

$$E = -\frac{\partial U}{\partial l} - j\omega A \tag{4}$$

On the other hand, the tangential electric field on the surface of a conductor, considering their self impedance per unit length z (Ω/m), gives:

$$E = zI \tag{5}$$

Combining (4) and (5), the following fundamental differential equation is obtained:

$$zI + j\omega A + \frac{\partial U}{\partial l} = 0 \tag{6}$$

Equation (6) is derived directly from the Maxwell equations and is then valid in all conditions, also non stationary. In practical cases, (6) can be solved only in a numerical way.

As anticipated, the conductor's network is partitioned into a suitable number of elements. Each element has to be very short if compared to both wavelength and system size. Therefore, the right elements number depends on propagation media, characteristic frequency of input source and grounding system size.

Each element is oriented from its start point (in) and its end point (out). Integrating (6) between the ends of an element, replacing the vector and scalar potential with (2) and rearranging, the following linear equation is obtained:

$$Z_i I_i + \sum_{j\neq i} M_{ij} I_j + \sum \left(W_{out\,ij} - W_{in\,ij}\right) J_j = 0 \tag{7}$$

where Z (Ω) is the self-impedance of the element, M (Ω) and W (Ω) are the partial mutual coupling and partial potential coefficients between elements respectively, I (A) and J (A) are longitudinal and leakage currents respectively.

The calculation of the self and mutual impedances and potential coefficient with a uniform and infinite extended propagation media is quite simple. In this case, the following equations can be used:

$$M_{ij} = \frac{j\omega\mu}{4\pi}\int_{in}^{out}\int_{in}^{out}\frac{e^{-\gamma r}}{r}dl_i dl_j \tag{8a}$$

$$W_{out\,ij} = \frac{\rho}{4\pi l}\int_{in}^{out}\frac{e^{-\gamma r}}{r}dl_j\Bigg|_{out} \tag{8b}$$

$$W_{in\,ij} = \frac{\rho}{4\pi l}\int_{in}^{out}\frac{e^{-\gamma r}}{r}dl_j\Bigg|_{in} \tag{8c}$$

The presence of a non-uniform media introduces a strong complexity in previous equations. As known, the rigorous and general formulation in the presence of a propagation media with a conducting half space involves Green functions and Sommerfeld integrals [1], [3]. At low frequency, simplifications can be introduced.

Writing a linear equation for each element, the Maxwell equations are then reduced to a linear system.

Each element is represented with a simplified "T" equivalent circuit as shown in Fig. 2.1 and introduces the following unknowns: input and output currents, and leakage current and potential of the middle point.

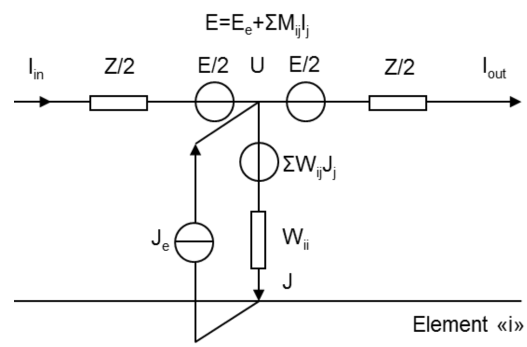

Fig. 2.1. Equivalent circuit of the generic element "i"

The resulting linear systems can be written as follows:

$$\begin{cases} \{U\} = [W]\{J\} \\ \{E_z\} + \{E_e\} = -\left([Z]+[M]\right)\{I\} \\ \{J\} = [A]\{I\} + \{J_e\} \end{cases} \tag{9}$$

where:
- $[W]$ = matrix of partial potential coefficient
- $[Z]$ = matrix of self-impedances
- $[M]$ = matrix of partial mutual impedances
- $[A]$ = incidence matrix
- $\{U\}$ = array of potentials
- $\{I\}$ = array of currents
- $\{J\}$ = array of leakage currents
- $\{E_z\}$ = array of voltage drops
- $\{E_e\}$ = array of forcing electromotive force
- $\{J_e\}$ = array of injected currents

The linear system (9), provides the distribution of currents, potentials and leakage currents along the conductor's network. From these main results, it is possible to calculate other important distributions as for instance: earth surface potentials and then touch and step voltages, electric and magnetic fields.

The calculation model above described is suitable for the frequency domain but also for the time domain by using the direct and inverse discrete Fourier transforms. As known a time domain transient can be considered as a superposition of many single frequency signals as follows:

$$s(t_n) = \frac{1}{N\Delta t_c} \sum_{k=0}^{N-1} S(f_k) e^{j\frac{2\pi nk}{N}} \quad n = 0, 1, \ldots N\text{-}1 \tag{10}$$

where:
- $s(t_n)$ = discrete Fourier transform
- $S(f_k)$ = coefficient of the nth harmonic
- N = sampling number
- Δt_c = sampling time interval

The $S(f_k)$ values can be calculated by using a direct discrete Fourier transform. In practical cases the maximum harmonics number in (10) is limited to N values depending on the frequency spectrum of the input transient.

The above described frequency domain model can be used for each harmonic and, at the end, N different output in the frequency domain will be obtained. The time domain output can be obtained from these outputs by using the inverse discrete Fourier transform.

Calculations in the time domain using a frequency domain approach (the described approach) if compared to the direct methods are characterized by increased accuracy because they are based strictly on the principles of electromagnetism, and the least errors are made [9]. Moreover, these methods allow considering the frequency dependence of the soil parameters in a rigorous way. The only requirement to apply this approach is the linearity of the model in the considered frequency range. These methods are anyway suitable also for nonlinear phenomena like soil ionization with accuracy acceptable for engineering applications.

III. Simulation of Finite Volumes

The simulation of low resistivity volumes is propaedeutic to the simulation of the sea effects. The sea will be represented with a very large finite volume, a virtually infinite volume.

A low resistivity finite volume can represent a buried tank, the basement of a building with reinforced concrete foundation or also a cavity full of sea water and so on.

If the resistivity of the finite volume is much lower than the soil resistivity, the finite volume can be simulate using a metal cage with the same shape of the external surface of the volume to simulate.

In order to make evident the effects of this finite volume, the scenario of Fig. 3.1 has been considered.

The grid size is 50 x 50 m with meshes 10 x 10 m and depth 1 m, the finite volume is a parallelepiped 50 x 20 x 10 m close to the soil surface. The minimum distance between grid and parallelepiped is 10 m. The current injected in the earth is 10 kA, the frequency is 60 Hz and the soil model is uniform with resistivity 100 Ωm and relative permittivity 6.

Without additional data input, the finite volume is assumed at floating potential. The program allows forcing the potential of the finite volume to zero, so to the potential of the remote earth.

The soil surface potential distributions on a rectangular area lying on the soil surface with and without the finite volume are represented in Fig. 3.2.

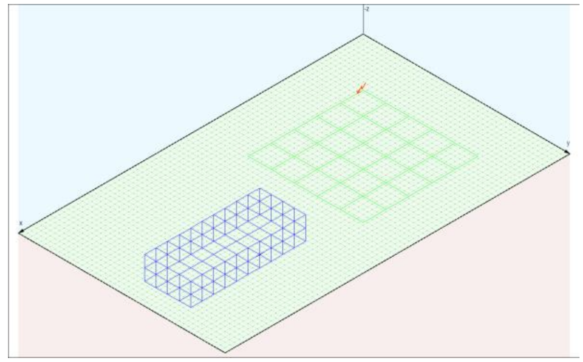

Fig. 3.1: Layout of grid (green) and finite volume (blue)

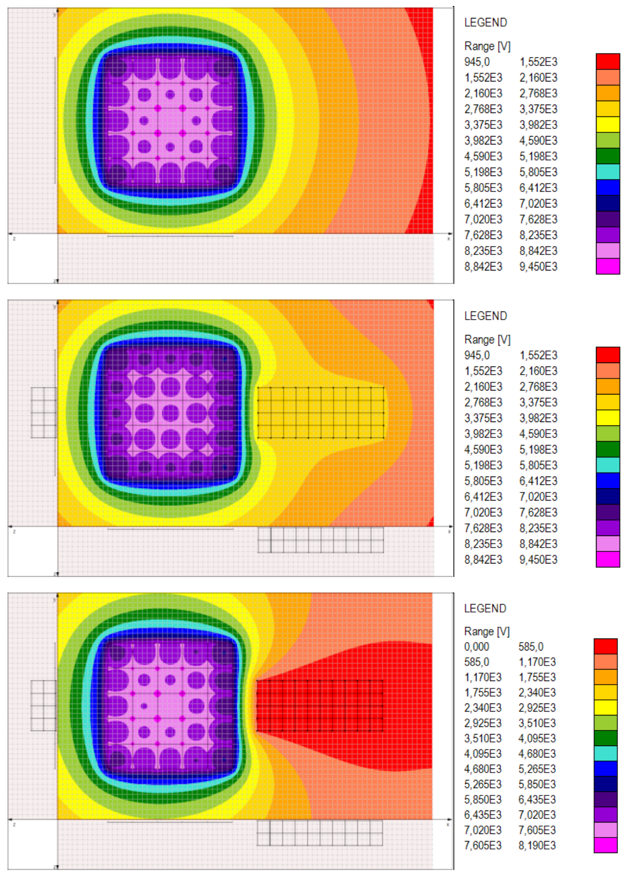

Fig. 3.2: Soil surface potential distributions
Upper without finite volume
Mid with floating finite volume
Bottom with finite volume at potential zero

The soil surface potential and touch and step voltages distributions on a line lying on the soil surface with and without the finite volume are represented in Fig. 3.3 and Fig. 3.4 (with the same scale of potential for convenience).

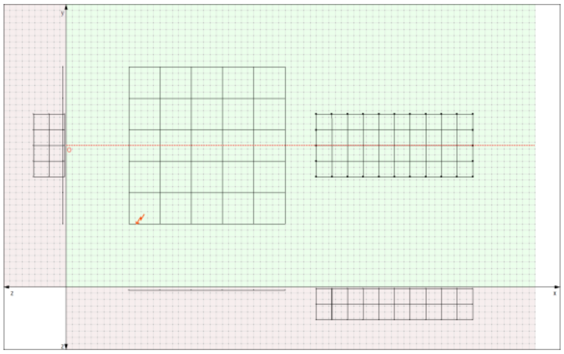

Fig. 3.3: Line calculation

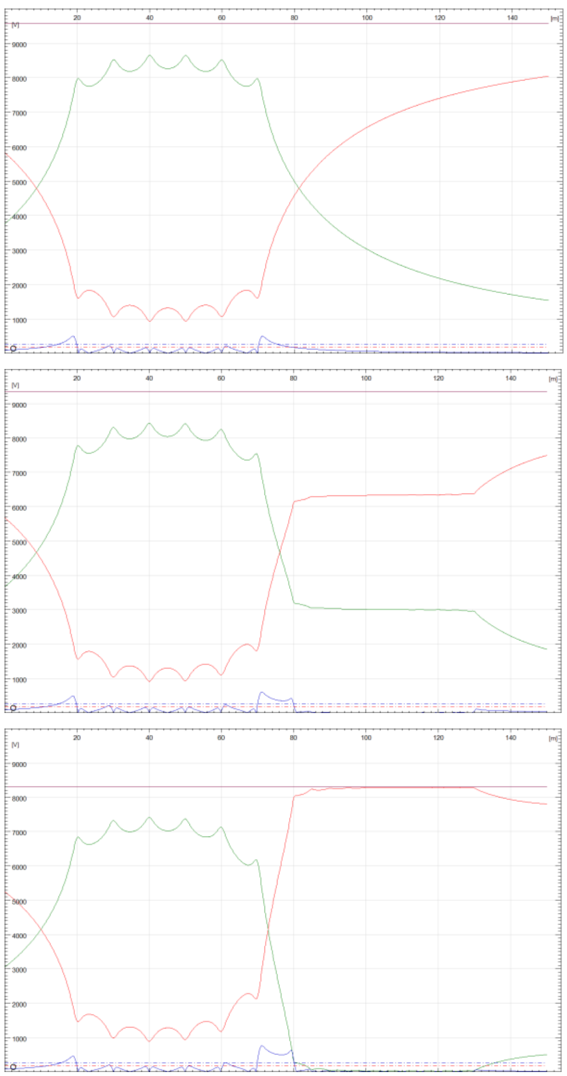

Fig. 3.4: Soil surface potential (green) and touch (red) and step (blue) voltages distributions
Upper without finite volume
Mid with floating finite volume
Bottom with finite volume at potential zero

The effects of the finite volume on soil surface potential and touch and step voltages distribution are evident from Fig. 3.2 and 3.4.

The GPR of the grounding system are: 9575 V without finite volume, 9341 V with finite volume at floating potential and 8303 V with finite volume at potential zero.

Overlapping the results in Fig. 3.4 without finite volume and with finite volume at potential zero the following results can be obtained: the touch voltages tend to grow in all peripheral parts of the grid, the step voltages tend to grow in the zones between grid and finite volume.

If the cage used to simulate the finite volume is at floating potential, the GPR of the cage (3014 V in the specific case) depends on the conductive coupling between grounding system and cage and then on their layout, mutual position and on soil resistivity. The total leakage current on the cage is of course null. The cage draws current from the ground near the grounding system and returns it far.

If the cage used to simulate the finite volume is at potential zero, the total leakage current on the cage in this case is not null.

The finite volume effects reduce when volume size decrease or when distance between grounding system and volume increases. The effects of the finite volume at potential zero is much stronger than when potential is floating.

This first case highlights the effects of a low resistivity finite volume close a grid in a simple case. Of course, the program can simulate more complex scenarios, with irregular layout of grounding system and finite volume, multiple grounding systems or finite volumes, multilayer or multizone soil model and so on. This will be shown in the following in order to simulate the effects of the sea in two typical cases.

IV. Sea Effects on Grounding Systems

The simulation of the sea effects on a grounding system close to the seacoast is very interesting for practical applications. The sea effects can be evident also when distance between grounding system and seacoast is significant. The study of the distance to which the sea effects are negligible requires a parametric study but in the first approximation, this distance is of the same order of magnitude of the system size.

If as usually happen, the resistivity of sea (about 0.20 Ωm) is much lower than the soil resistivity, the sea can be simulated using a metal grid with the same shape of the seabed extended up to a distance a few times the maximum size of the system.

The grid potential can be imposed null, as the remote earth. The scenario of Fig. 4.1 has been considered.

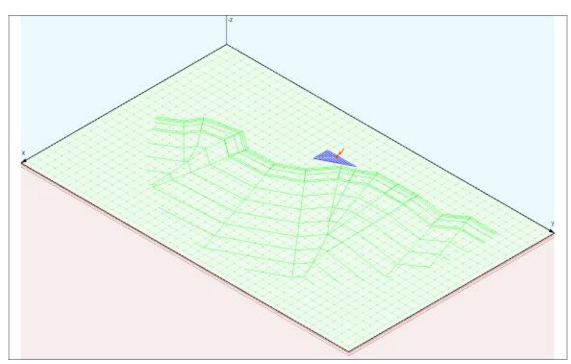

Fig. 4.1: Layout of grid (blue) and seabed (green)

The grid is triangular with a maximum size about 200 m and depth 1 m and a minimum distance to the seacoast about 40 m. The current injected in the earth is 5 kA, the frequency is 60 Hz and the soil model is a four layer soil model with the following parameters (see Fig. 4.2):

Layer 1: resistivity = 100.0 Ωm, thickness = 2.000 m
Layer 2: resistivity = 50.00 Ωm, thickness = 6.000 m
Layer 3: resistivity = 200.0 Ωm, thickness = 15.00 m
Layer 4: resistivity = 75.00 Ωm

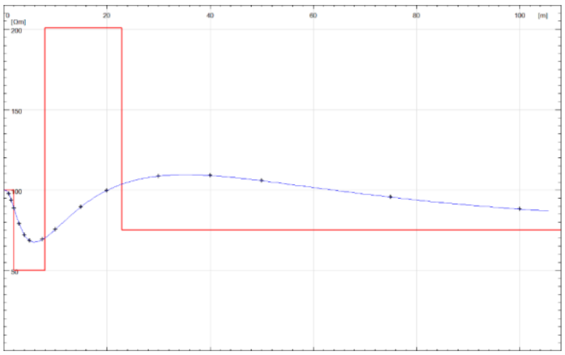

Fig. 4.2: Apparent soil resistivity of the used four layers soil model

The soil surface potential and touch and step voltages distributions on a line lying on the soil surface with and without sea are represented in Fig. 4.4 and Fig. 4.5 (with the same scale of potential for convenience).

The GPR of the grounding system is 1906 V and 1662 V without and with sea respectively.

The effects of the sea on the earth surface potential and touch and step voltages distribution are evident from Fig. 4.5.

Overlapping the results in Fig. 4.5 without and with sea the following results can be obtained: the touch voltages tend to grow in all peripheral parts of the grid, the step voltages tend to grow only close to the seacoast. The step voltages can grow in all areas between grid and seacoast if the distance between grid and seacoast is much lower but anyway with values seldom dangerous.

The sea effects are quite evident if the calculation is performed using a constant current to earth but is more evident if the calculation is performed using a constant GPR.

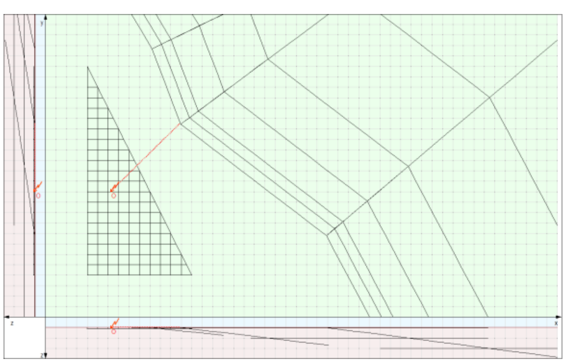

Fig. 4.4: Line calculation

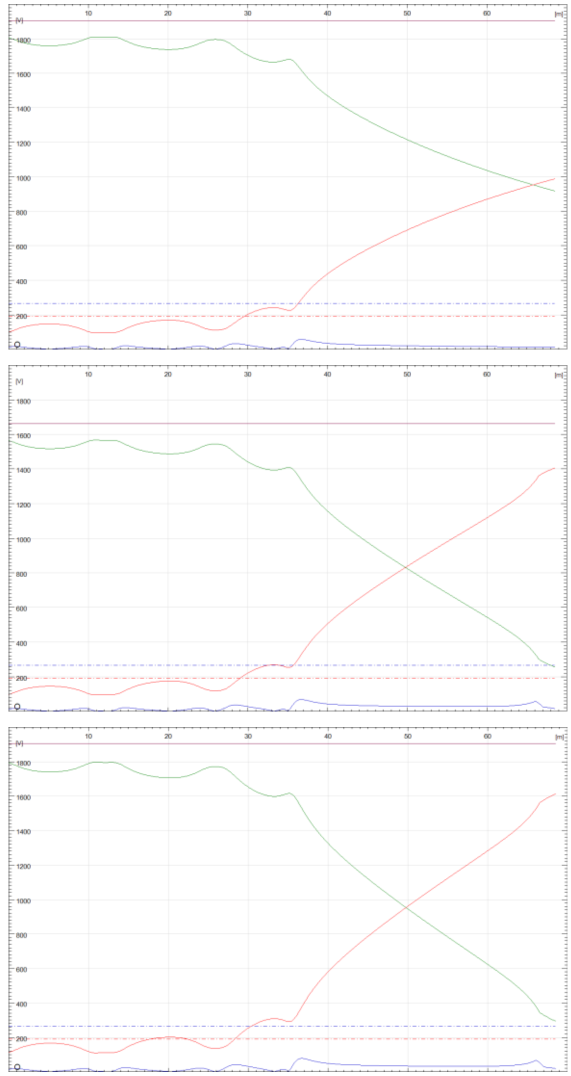

Fig. 4.5: Soil surface potential (green) and touch (red) and step (blue) voltages distributions
Upper without sea
Mid with sea and constant current
Bottom with sea and constant GPR

This is also evident in Fig. 4.6. where the safe areas without and with sea are represented.

In Fig. 4.6 a clearing time 0.5 s and a body weight 50 kg has been considered, so the permissible touch and step voltages according to the IEEE Std 80 – 2013 are 189.7 V and 266.8 V respectively.

In the specific case, the safe conditions are related only to the touch voltages because as usual, step voltages are not dangerous.

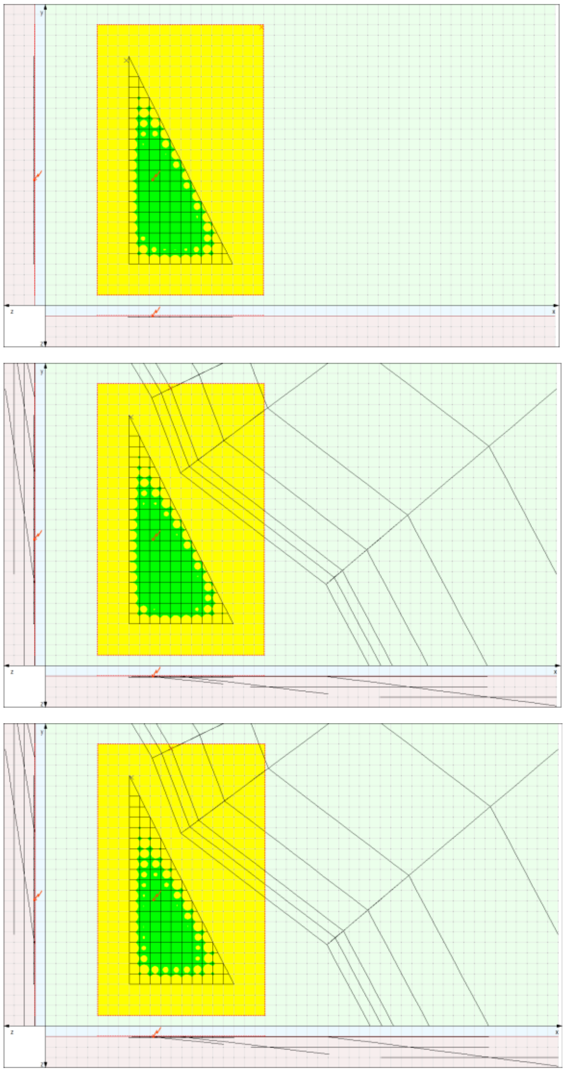

Figure 4.6: Safe areas (green)
Upper without sea
Mid with sea and constant current
Bottom with sea and constant GPR

V. Sea Effects on Cathodic Protection Plants

Cathodic protection is one of the most used methods to prevent or limit the corrosion of buried or submerged metals.

Cathodic protection uses a flow of direct current to interfere with the activity of the electrochemical cells responsible for corrosion. Corrosion is prevented by coupling the metal being protected with a more active metal when both are immersed in an electrolyte and connected with an external path. In this case, the entire surface of the metal being protected becomes a cathode, thus the term “cathodic protection”.

The current flow can be provided by a source commonly called anode. Anode made from active metal are commonly called “sacrificial”, as the anode material is sacrificed to protect the structure under protection. Anode made from inert metal are commonly called “impressed current anodes”, as an external energy source is used to impress a current onto the structure under protection. The cathodic protection plants with impressed currents are the preferred when systems to be protected are large.

The operative criterion for cathodic protection consists in forcing the potential on the system surface within a given range, for example “-900 mV < U < -350 mV”. This can be obtained by suitably positioning the anodes and suitably adjusting the protection current. Under protection implies corrosion but also overprotection implies damages to the pipeline.

In Fig. 5.1 is represented a long pipeline (length > 150 km) and the corresponding multizone soil model (with 35 zones) without considering the presence of the sea.

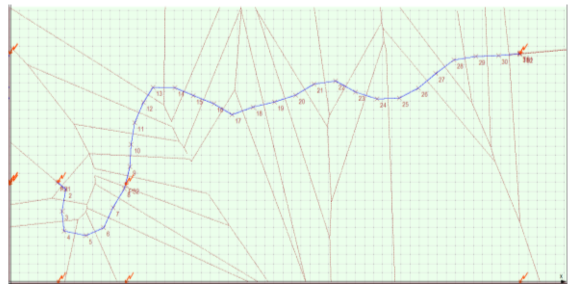

Fig. 5.1: Layout of pipeline (blue), multizone soil model without sea and cathodic protection plants

The pipeline can be protected by using only three feeders placed for instance as represented in the Fig. 5.1 with a red flash. The distribution of the potential along the pipeline is represented in Fig. 5.2a and 5.2b.

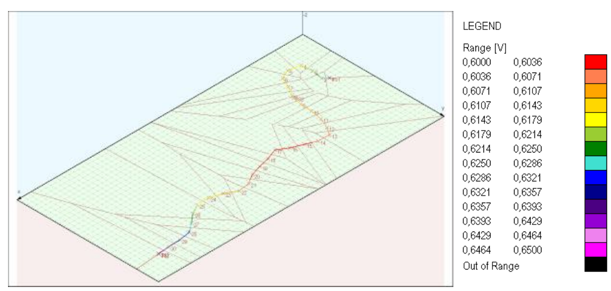

Fig. 5.2a: Potential distribution

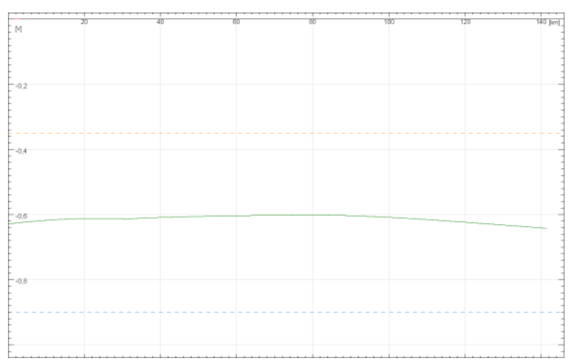

Fig. 5.2b: Potential distribution without sea

The potentials distribution meets the criterion “-900 mV < V < -350 mV”, so the pipeline is correctly protected.

Now the effects of the sea are included in simulations. In Fig. 5.3 is represented the same scenario considering the presence of the sea.

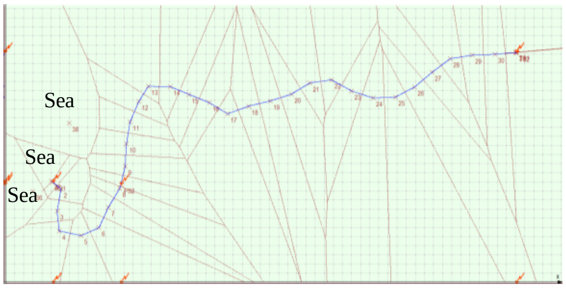

Fig. 5.3: Layout of pipeline (blue) and multizone soil model with sea

In the same conditions (same anodes and same protection currents), the distribution of the potential along the pipeline is represented in Fig. 5.4.

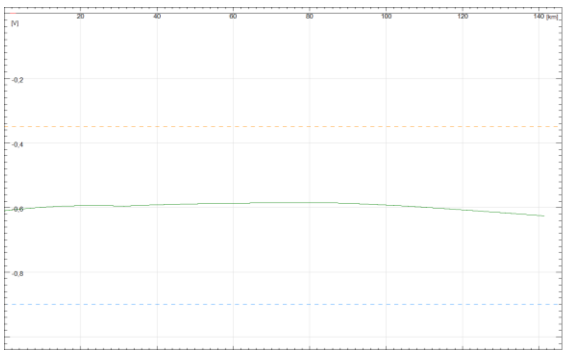
Fig. 545: Potential distribution with sea

The sea effects are negligible on potential distribution. This because assuming a constant impressed current, the pipeline potential is related mainly to the coating effects and the effects of soil resistivity is limited. The presence of the sea has no significant effects on the distribution of potential on the pipeline.

VI. Conclusion

This paper presents a study of the sea effects on grounding systems close to the seacoast. The numerical study has been extended also to the sea effects on cathodic protection systems because of great interest on real-life applications.

The paper shows how modern programs are able to represent a complex scenario with grounding systems with any shape, buried in soil represented with a multilayer or multizone model close to the seacoast with an arbitrary shape of the seabed in a very realistic way.

The sea effects are usually evident depending on soil resistivity, grounding system shape and in particular on distance to the seacoast. The simulation of the sea effects is in general required when distance between grounding system and seacoast is of the same order of magnitude of the system size.

If the calculation is performed assuming a constant current to earth, the presence of the sea reduces the GPR of the grounding system but surprisingly, it increases touch voltages in all peripheral parts of the grid. If the calculation is performed assuming a constant GPR value, the increasing of the touch voltages can be relevant.

The effects of the sea in the step voltages are evident only in the area between grounding system and seacoast and only if the distance between grid and seacoast is limited.

The paper confirms the importance of a realistic simulation of the sea effects when a grounding system lie close to the seacoast.

The only requirement for the simulation of the sea is that the sea resistivity is much lower than the soil resistivity, as usually happen. In this case, simulation can be very realistic.

Conversely, sea effects are substantially negligible on potential distribution along an insulated pipeline protected with a cathodic protection system. In these cases, assuming a constant impressed current, the presence of the sea if not relevant in results.

VII. References

[1] E.D. Sunde, Earth Conduction Effects in Transmission Systems, first ed., D. Van Nostrand Company Inc., New York, 1949.

[2] G. F. Tagg, Earth Resistance, first ed., George Newnes Limited, London, 1964.

[3] S. Ramo, J.R. Whinnery, T. Van Duzer, Fields and Waves in Communication Electronics, first ed., Wiley International Edition, New York and London, 1965.

[4] A. Banos, Dipole Radiation in the Presence of a Conductive Half-Space, first ed., Pergamon Press Inc., Oxford – London – Edinburgh - New York, Paris and Frankfurt, 1966

[5] R. G. Van Nostrand, K. L. Cook, Interpretation of Resistivity Data, first ed., United States Government Printing Office, Washington: 1984

[6] R. Andolfato, L. Bernardi, L. Fellin, Aerial and Grounding System Analysis by the Shifting Complex Images Method, IEEE Transactions on Power Delivery, Vol. 15, No. 3, July 2000, pp. 1001 – 1009.

[7] R. Alipio, S. Visacro, Frequency Dependence of Soil Parameters: Effect on the Lightning Response of Grounding Electrodes, IEEE Transactions on Electromagnetic Compatibility, 2012

[8] R. Alipio, S. Visacro, Frequency Dependence of Soil Parameters: Experimental Results, Predicting Formula and Influence on the Lightning Response of Grounding Electrode, IEEE Transactions on Power Delivery, Vol. 27, no. 2, April 2012

[9] J. He, R. Zeng, B.Zhang, Methodology and Technology for Power System Grounding, first ed., John Wiley & Sons Singapore Pte. Ltd., 2013

[10] CIGRE WG C4.501 June 2013 “Guideline for Numerical Electromagnetic Analysis Method and its Application to Surge Phenomena”

[11] J. Q. Keji Chen, J. Xu, X. Wen, Z. Pan, Q. Yang, Comparative Study of Different Parameter Inversion Methods, Proceedings of the World Congress on Engineering and Computer Science 2014 Vol I, WCECS 2014, 22-24 October, 2014, San Francisco, USA

[12] D. Cavka, N. Mora, F. Rachidi, A Comparison of Frequency Dependent Soil Models: Application to the Analysis of Grounding Systems, IEEE Transactions on Electromagnetic Compatibility, Vol. 56, no. 1, February 2014

[13] IEEE Std 80™-2013 “IEEE Guide for Safety in AC Substation Grounding”

[14] “XGSLab™ rel. 8.3.1 User’s Guide” SINT Ingegneria Srl.

[15] “XGSLab™ rel. 8.3.1 Tutorials” SINT Ingegneria Srl.

VIII. Biographies

Arturo Bretas is a professor at the department of electrical and computer engineering of the University of Florida. His research interests include power systems operation, protection and control. He has held visiting positions at universities all over the world, including the Grenoble Institute of Technology, Grenoble France during 2003-2004 where he was a CNRS Scholar. Since 2002, he has been involved as a PI/CPI on more than 17 RD&D projects funded by the industry and the government. These projects concern, for example, cyber-physical system security, new technologies to enhance power system control and monitoring, distribution systems reliability optimization and planning under deregulation. Dr. Bretas has published up to date more 253 scientific papers in international conferences and journals.

Roberto Andolfato received a Dr. Ing. and Ph.D. degree in electrical engineering from University of Padua, Italy in 1990 and 1998, respectively. He is an invited lecturer of structured seminars at the University of Padua. His main fields of interest are grounding systems and electric and magnetic fields, with specific emphasis on developing numerical procedures for simulating the electromagnetic field generated by complex geometry in dispersing media or in the air, in both frequency and time domain. He is also a Professional Consultant Engineer and a member of the Italian Electrical and Electronic Association (AEIT). Dr. Andolfato has published up to date more 16 scientific papers in international conferences and journals.

Daniele Cuccarollo received a Dr. Ing. degree in electrical engineering from University of Padua, Italy in 2009. His main fields of interest are grounding systems and electric and magnetic fields, with specific emphasis on developing numerical procedures for simulating the electromagnetic field generated by complex geometry in dispersing media and in the air in both frequency and time domain.